



Genomic Diversity and Evolution of the Head Crest in the Rock Pigeon

Michael D. Shapiro *et al.*
Science **339**, 1063 (2013);
DOI: 10.1126/science.1230422

This copy is for your personal, non-commercial use only.

If you wish to distribute this article to others, you can order high-quality copies for your colleagues, clients, or customers by [clicking here](#).

Permission to republish or repurpose articles or portions of articles can be obtained by following the guidelines [here](#).

The following resources related to this article are available online at www.sciencemag.org (this information is current as of March 4, 2013):

Updated information and services, including high-resolution figures, can be found in the online version of this article at:

<http://www.sciencemag.org/content/339/6123/1063.full.html>

Supporting Online Material can be found at:

<http://www.sciencemag.org/content/suppl/2013/01/30/science.1230422.DC1.html>

This article **cites 61 articles**, 31 of which can be accessed free:

<http://www.sciencemag.org/content/339/6123/1063.full.html#ref-list-1>

This article appears in the following **subject collections**:

Evolution

<http://www.sciencemag.org/cgi/collection/evolution>

enrichment, should be paced by changes in dust concentration. During TIII, the change in dust occurs earlier than the change in ice isotope at both EDC and Vostok (figs. S7 and S8), whereas these two records are approximately in phase during TI (fig. S8). This could explain why the Vostok $\delta^{40}\text{Ar}$ record is in advance with respect to the aCO_2 record, without contradicting our finding of synchronous changes in aCO_2 and AT. During TII at EDC (fig. S8), on the other hand, the change in $\delta^{15}\text{N}$ occurs at a deeper depth than the change in dust. Dust concentration therefore cannot be the only factor influencing the LID.

Our results are also in general agreement with a recent 0- to 400-year aCO_2 -AT average lag estimate for TI (20), using a different approach. Although this study does not make any assumption about the convective zone thickness, it is based on coastal cores, which might be biased by local changes in ice sheet thickness; and firn densification models, which may not be valid for past conditions (see the supplementary materials for a more detailed discussion).

Our chronology and the resulting aCO_2 -AT phasing strengthens the hypothesis that there was a close coupling between aCO_2 and AT on both orbital and millennial time scales. The aCO_2 rise could contribute to much of the AT change during TI, even at its onset, accounting for positive feedbacks and polar amplification (21), which magnify the impact of the relatively weak rCO_2 change (Fig. 4) that alone accounts for $\sim 0.6^\circ\text{C}$ of global warming during TI (21). Invoking changes in the strength of the Atlantic meridional overturning circulation is no longer required to explain the lead of AT over aCO_2 (22).

Given the importance of the Southern Ocean in carbon cycle processes (23), one should not exclude the possibility that aCO_2 and AT are interconnected through another common mechanism such as a relationship between sea ice cover and ocean stratification. Although the tight link between aCO_2 and AT suggests a major common mechanism, reviews of carbon cycle processes suggest a complex association of numerous independent mechanisms (2, 23).

Changes in aCO_2 and AT were synchronous during TI within uncertainties. Our method, based on air ^{15}N measurements to determine the ice/gas depth shift, is currently being used in the construction of a common and optimized chronology for all Antarctic ice cores (24, 25). The assumption that no convective zone existed at EDC during TI might be tested in the future by using Kr and Xe isotopes (26). Further studies on the firn are needed to understand the causes of the past variations of the LID, such as the possible impact of impurity concentrations on the densification velocity. Although our study was focused on the relative timing of TI climatic records extracted from Antarctic ice cores, there is now the need to build a global chronological framework for greenhouse gases, temperature reconstructions, and other climate proxies at various locations (22). Although the timings of the Bølling, Younger Dryas,

and Holocene onsets as visible in the methane records are now well constrained by a layer-counted Greenland chronology (27), determining the timing of the onset of TI in Antarctic records remains challenging. Modeling studies using coupled carbon cycle–climate models will be needed to fully explore the implications of this synchronous change of AT and aCO_2 during TI in order to improve our understanding of natural climate change mechanisms.

References and Notes

1. E. Monnin *et al.*, *Science* **291**, 112 (2001).
2. A. Lourantou *et al.*, *Global Biogeochem. Cycles* **24**, GB2015 (2010).
3. H. Fischer, M. Wahlen, J. Smith, D. Mastroianni, B. Deck, *Science* **283**, 1712 (1999).
4. L. Loulergue *et al.*, *Clim. Past* **3**, 527 (2007).
5. F. Parrenin *et al.*, *Clim. Past* **8**, 1239 (2012).
6. C. Goujon, J.-M. Barnola, C. Ritz, *J. Geophys. Res.* **108**, ACL10/1-10 (2003).
7. F. Parrenin *et al.*, *Clim. Past* **3**, 243 (2007).
8. H. Craig, Y. Horibe, T. Sowers, *Science* **242**, 1675 (1988).
9. T. A. Sowers, M. Bender, D. Raynaud, Y. L. Korotkevich, *J. Geophys. Res.* **97**, 15683 (1992).
10. A. Landais *et al.*, *Quat. Sci. Rev.* **25**, 49 (2006).
11. G. B. Dreyfus *et al.*, *Quat. Sci. Rev.* **29**, 28 (2010).
12. J. P. Severinghaus *et al.*, *Earth Planet. Sci. Lett.* **293**, 359 (2010).
13. T. F. Stocker, S. J. Johnsen, *Paleoceanography* **18**, 1 (2003).
14. G. M. Raisbeck, F. Yiou, J. Jouzel, T. F. Stocker, *Clim. Past* **3**, 541 (2007).
15. S. Barker *et al.*, *Science* **334**, 347 (2011).
16. M. Hörhold *et al.*, *Earth Planet. Sci. Lett.* **325–326**, 93 (2012).
17. P. Köhler, G. Knorr, D. Buiron, A. Lourantou, J. Chappellaz, *Clim. Past* **7**, 473 (2011).
18. G. Myhre, E. J. Highwood, K. P. Shine, F. Stordal, *Geophys. Res. Lett.* **25**, 2715 (1998).
19. N. Caillon *et al.*, *Science* **299**, 1728 (2003).
20. J. B. Pedro, S. O. Rasmussen, T. D. van Ommen, *Clim. Past* **8**, 1213 (2012).

21. P. Köhler *et al.*, *Quat. Sci. Rev.* **29**, 129 (2010).
22. J. D. Shakun *et al.*, *Nature* **484**, 49 (2012).
23. H. Fischer *et al.*, *Quat. Sci. Rev.* **29**, 193 (2010).
24. L. Bazin *et al.*, *Clim. Past Discuss.* **8**, 5963 (2012).
25. D. Veres *et al.*, *Clim. Past Discuss.* **8**, 6011 (2012).
26. J. P. Severinghaus, A. Grachev, B. Luz, N. Caillon, *Geochim. Cosmochim. Acta* **67**, 325 (2003).
27. A. Svensson *et al.*, *Clim. Past* **4**, 47 (2008).
28. J. Jouzel *et al.*, *Science* **317**, 793 (2007).
29. L. Loulergue *et al.*, *Nature* **453**, 383 (2008).

Acknowledgments: We thank O. Watanabe, B. Stenni, and EPICA community members for giving access to, respectively, the DF1, TALDICE, and EDM1 isotopic data; L. Loulergue, D. Buiron, and T. Blunier for giving access to, respectively, the EDC-EDML, TALDICE, and GRIP CH_4 data; G. Dreyfus for giving access to the $\delta^{15}\text{N}$ isotopic data; and G. Delaygue, J. Chappellaz, S. Barker, and A. Ganopolski for helpful discussions. This work greatly benefited from constructive comments by two anonymous reviewers. This work had support from the French Agence Nationale de la Recherche (project ANR-07-BLAN-0125 "Dome A" and ANR-09-SYSC-001 "ADAGE"). This work is a contribution to EPICA, a joint European Science Foundation/European Commission scientific program, funded by the European Union and by national contributions from Belgium, Denmark, France, Germany, Italy, the Netherlands, Norway, Sweden, Switzerland, and the United Kingdom. Main logistical support was provided by the Institut Paul Emile Victor and the Programma Nazionale Ricerche in Antartide at Dome C. We thank the technical teams in the field and at the different laboratories. This is EPICA publication no. 291.

Supplementary Materials

www.sciencemag.org/cgi/content/full/339/6123/1060/DC1
Materials and Methods
Supplementary Text
Figs. S1 to S8
Tables S1 to S7
Database S1

20 June 2012; accepted 9 January 2013
10.1126/science.1226368

Genomic Diversity and Evolution of the Head Crest in the Rock Pigeon

Michael D. Shapiro,^{1*} Zev Kronenberg,² Cai Li,^{3,4} Eric T. Domyan,¹ Hailin Pan,³ Michael Campbell,² Hao Tan,³ Chad D. Huff,^{2,5} Haofu Hu,³ Anna I. Vickrey,¹ Sandra C. A. Nielsen,⁴ Sydney A. Stringham,¹ Hao Hu,⁵ Eske Willerslev,⁴ M. Thomas P. Gilbert,^{4,6} Mark Yandell,² Guojie Zhang,³ Jun Wang^{3,7,8*}

The geographic origins of breeds and the genetic basis of variation within the widely distributed and phenotypically diverse domestic rock pigeon (*Columba livia*) remain largely unknown. We generated a rock pigeon reference genome and additional genome sequences representing domestic and feral populations. We found evidence for the origins of major breed groups in the Middle East and contributions from a racing breed to North American feral populations. We identified the gene *EphB2* as a strong candidate for the derived head crest phenotype shared by numerous breeds, an important trait in mate selection in many avian species. We also found evidence that this trait evolved just once and spread throughout the species, and that the crest originates early in development by the localized molecular reversal of feather bud polarity.

Since the initial domestication of the rock pigeon in Neolithic times (1), breeders have selected striking differences in behavior, vocalizations, skeletal morphology, feather ornaments, colors, and color patterns to establish over 350 breeds (2). In many cases, the number and magnitude of differences among breeds are

more characteristic of macroevolutionary changes than of changes within a single species (2, 3). Indeed, Charles Darwin was so fascinated by domestic pigeons that he repeatedly called attention to this dramatic example of diversity within a species to communicate his ideas about natural selection (3, 4).

The genetic architecture for many derived traits in pigeons is probably relatively simple (5, 6), probably more so than that for interspecific trait variation among many wild species,

because breeders often focus on qualitative rather than quantitative variation; this increases the chance of identifying genes responsible for differences among breeds. Additionally, several morphological traits show similar patterns of variation in different breeds, making it possible to test whether the same or different genes underlie similar phenotypes. Despite these advantages, the pigeon is underused as a model for the molecular genetic basis of avian variation because of the paucity of genetic and genomic resources for this bird.

We examined genomic diversity, genetic structure, and phylogenetic relationships among domestic breeds and feral populations (free-living birds descended from escaped domestics) of the rock pigeon. The pigeon reference genome was sequenced from a male Danish tumbler with the Illumina HiSeq 2000 platform, and we also resequenced 40 additional *Columba livia* genomes

to 8- to 26-fold coverage (38 individuals from 36 domestic breeds and two feral pigeons) (7). Genome-wide nucleotide diversity in the rock pigeon ($\pi = 3.6 \times 10^{-3}$) and the mutation rate estimate in the pigeon lineage (1.42×10^{-9} substitutions per site per year $\pm 2.60 \times 10^{-12}$ SE) are comparable to those of other avian species (8, 9). The observed heterozygosity indicates a large effective population size for the rock pigeon of $N_e \approx 521,000$; demographic inferences based on the allele frequency spectrum indicate that, aside from a very recent bottleneck, N_e has been remarkably stable over the past 1.5 million generations (7).

Patterns of linkage disequilibrium (LD) are indicative of haplotype sizes and genome-wide recombination rates and inform decisions about genetic mapping strategies. Using genotype data from the 40 resequenced *C. livia* genomes, we

¹Department of Biology, University of Utah, Salt Lake City, UT 84112, USA. ²Department of Human Genetics, University of Utah, Salt Lake City, UT 84112, USA. ³BGI-Shenzhen, Shenzhen, 518083, China. ⁴Centre for GeoGenetics, Natural History Museum of Denmark, University of Copenhagen, Øster Voldgade 5-7, 1350 Copenhagen, Denmark. ⁵Department of Epidemiology, University of Texas M. D. Anderson Cancer Center, Houston, TX 77030, USA. ⁶Ancient DNA Laboratory, Murdoch University, Perth, Western Australia 6150, Australia. ⁷Department of Biology, University of Copenhagen, DK-1165 Copenhagen, Denmark. ⁸Novo Nordisk Foundation Center for Basic Metabolic Research, University of Copenhagen, DK-1165 Copenhagen, Denmark.

*To whom correspondence should be addressed. E-mail: mike.shapiro@utah.edu (M.D.S.); wangj@genomics.org.cn (J.W.)

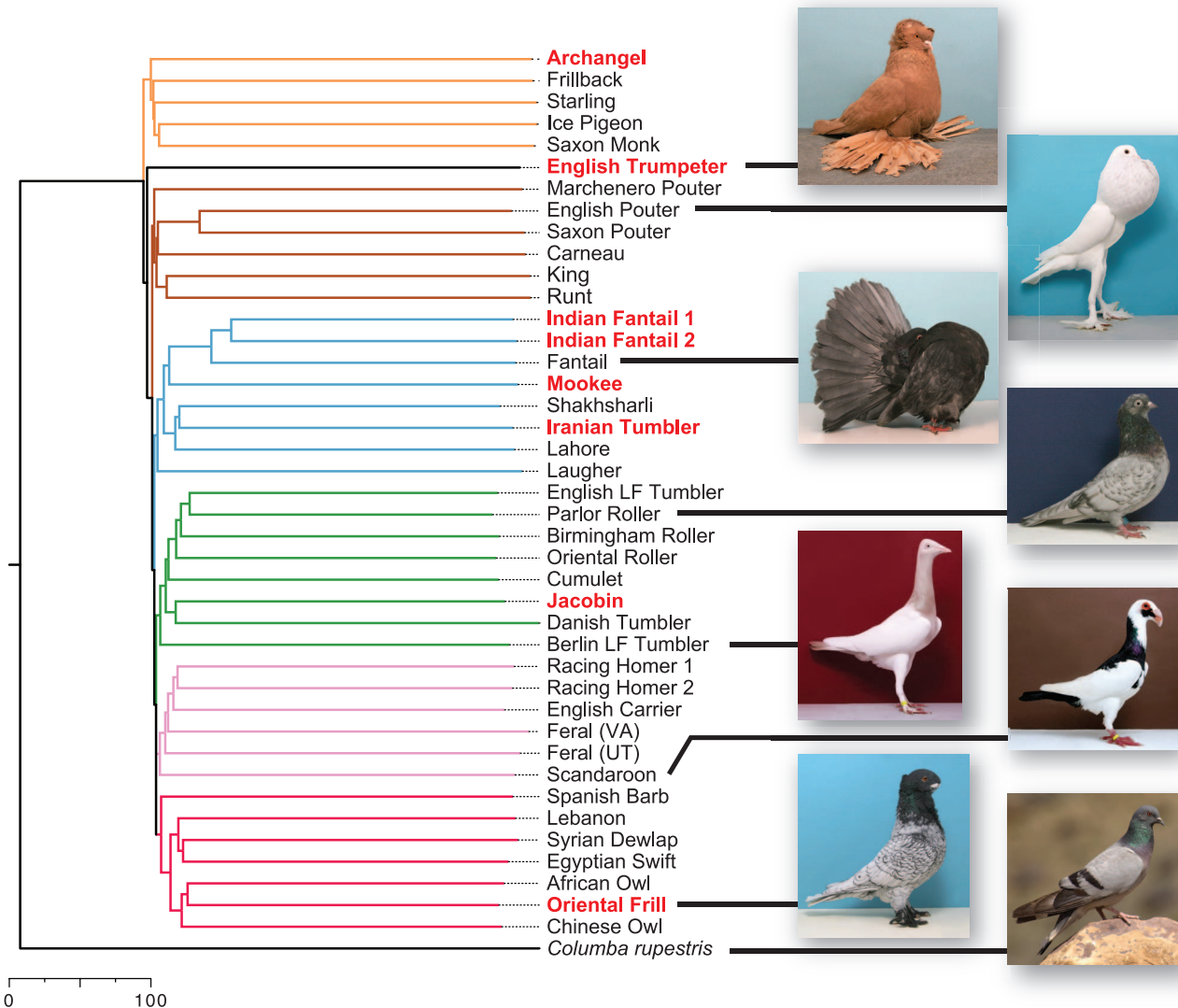


Fig. 1. Relationships among rock pigeons and the hill pigeon *C. rupestris*. A consensus neighbor-joining tree based on 1.48 million genomic SNPs and 1000 bootstrap replicates (see fig. S16 for bootstrap support) is shown. Branches are colored according to traditional breed groups (12) and/or geographic affinities: orange, toy breeds; brown, pouters and utility breeds;

light blue, Indian and Iranian breeds; green, tumblers and highflyers; pink, homers and wattle breeds; red, Mediterranean and owl breeds; black, voice characteristics (14). Bold red lettering indicates breeds with the head crest phenotype. Scale bar, Euclidean distance. [Photo credits: T. Hellmann (domestic breeds) and M. V. Shreeram (*C. rupestris*)]

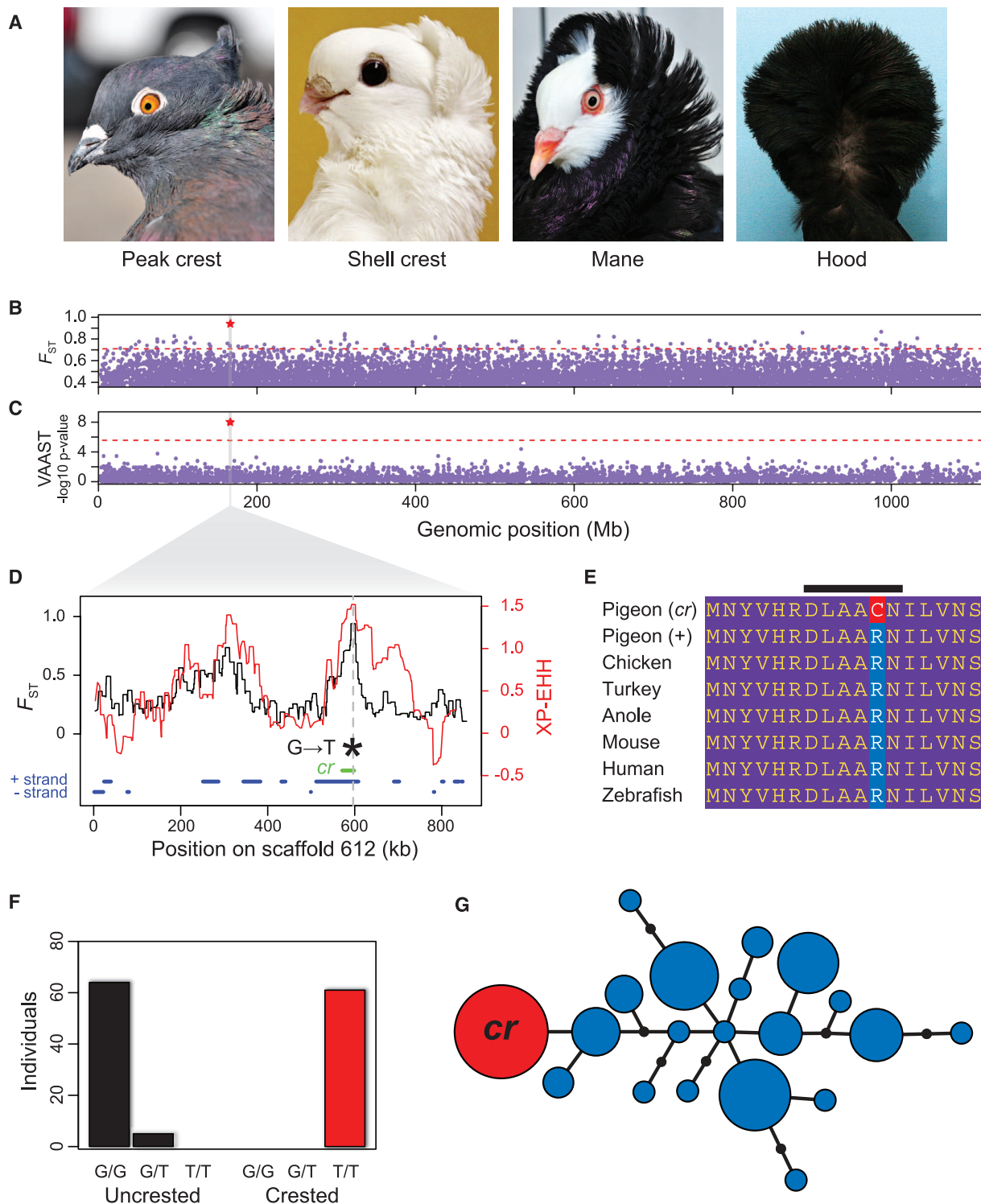


Fig. 2. *EphB2* is associated with the derived head crest phenotype. **(A)** Head crests are variable among breeds (left to right: Indian fantail, Old German owl, Old Dutch capuchin, Jacobin). **(B)** F_{ST} between crested and uncrested pigeons, with maximum value for individual SNPs plotted for nonoverlapping 100-kb windows across the genome. Red star, window with the highest score. Dashed red line, top 1% of scores. **(C)** Genome-wide VAAST scan. Each dot represents a single gene. Red star, gene with the highest score. Dashed red line, genome-wide significance cutoff. **(D)** Magnification of scaffold 612 in shaded region of (B) and (C). Black trace, maximum F_{ST} between crested and uncrested birds over a 300-SNP window. Red trace, unstandardized cross-population extended haplotype homozygosity (XP-EHH); higher values are evidence of selection (see fig. S21, genome-wide plot). Dashed

vertical line, position of the lone genome-wide significant VAAST hit. Green bar, the 27.4-kb haplotype shared by all crested birds, includes only the *EphB2* gene. Blue bars, gene predictions on + and - DNA strands. **(E)** The *cr* mutation induces a charge-changing amino acid substitution; black bar, highly conserved DLAARN motif of catalytic loop. **(F)** Genotypes of 159 birds from 79 breeds at the *cr* locus are perfectly associated with the crest phenotype under a recessive model. **(G)** Network diagram of the minimal 11-kb haplotype shared by all resequenced rock pigeons with the *cr* mutation (also see fig. S23). Many haplotypes contain the + allele (blue), but only one contains the *cr* SNP (red). The sizes of the circles are proportional to the number of chromosomes containing a haplotype. Line segments represent single-nucleotide differences. [Jacobin photo credit: T. Hellmann]

found that mean “useful LD” (10) (coefficient of determination, $r^2 > 0.3$) decays in 2.2 kb (fig. S10J). This suggests that we should expect little LD between typical pairs of genes in an analysis across breeds; thus, the pigeon is well suited for association-mapping strategies.

We leveraged our whole-genome data to determine breed relationships, using 1.48 million variable loci. A neighbor-joining tree rooted on *C. rupestris*, the sister species of *C. livia* (11), yielded several well-supported groups (Fig. 1 and fig. S16). Notably, the two feral pigeons grouped with the wattle and homer breeds (Fig. 1, pink branches), supporting the idea that escaped racing homers are probably major contributors to feral populations (12). As with many domesticated species, pigeon evolution is probably not exclusively linear or hierarchical (12). We therefore examined genetic structure among breeds by analyzing 3950 loci with ADMIXTURE (13) and found a best model fit at $K = 1$ (a single population, where K is the number of assumed ancestral populations). However, higher values of K can also be biologically informative (figs. S17 to S20). Our analysis includes some of the oldest lineages of domestic pigeons and breeds that were not exported from the Middle East until the late 19th or early 20th centuries (14), providing information about likely geographic origins of breeds and their exchange along ancient trade routes (7).

Derived traits in domesticated birds tend to evolve along a predictable temporal trajectory, with color variation appearing in the earliest stages of domestication, followed by plumage and structural (skeletal and soft tissue) variation, and finally behavioral differences (2). One of the genetically simplest derived traits of pigeons is the head crest. Head crests are common ornaments in many bird species (2) and are important display structures in mate selection (15). In pigeons, head crests consist of neck and occipital feathers with reversed growth polarity, so that the feathers grow toward the top of the head instead of down the neck. Crests can be as small and simple as a peak of feathers or as elaborate as the hood of the Jacobin, which envelops the head (Fig. 2A). Classical genetics experiments suggest that the head crest segregates as a simple Mendelian recessive trait (6, 14). Moreover, previous studies suggest that the same locus controls the presence of a crest in numerous breeds, either with alternative alleles at this locus or additional modifier loci controlling the extent of crest development (6, 14).

We resequenced eight individuals with head crests to directly test whether the same mutation controls crest development in different breeds. We sorted genomic variants from birds with and without head crests into separate bins and calculated allele frequency differentiation (F_{ST}) across the genome (Fig. 2B). We identified a region of high differentiation between crested and uncrested birds in the pigeon ortholog of *Ephrin receptor B2* (*EphB2*; $F_{ST} = 0.94$, top hit genome-wide;

fig. S22A) (Fig. 2D). The role of *EphB2* in feather growth is not known, but it plays important roles in tissue patterning and morphogenesis and is a member of a receptor tyrosine kinase family that mediates development of the feather cytoskeleton (16, 17). All eight crested birds were homozygous for a T nucleotide at scaffold 612, position 596613 (hereafter, the *cr* allele), whereas uncrested birds were heterozygous ($n = 3$) or homozygous ($n = 30$, including the uncrested outgroup *C. rupestris*) for the putatively ancestral C nucleotide (the + allele). These results were consistent with the known simple recessive architecture of the trait and implicated a common polymorphism associated with head crest development in multiple breeds with different genetic histories (Fig. 1). This trend extended well beyond our resequencing panel: We genotyped an additional 61 crested birds from 22 breeds and 69 uncrested birds from 57 breeds, and found a perfect association between *cr/cr* genotype and the crest phenotype (Fig. 2F). By treating the genomes of crested and uncrested birds as separate populations, we also found suggestive evidence for positive selection around the *cr* allele using cross-population extended haplotype homozygosity analysis (Fig. 2D and figs. S21 and S22B).

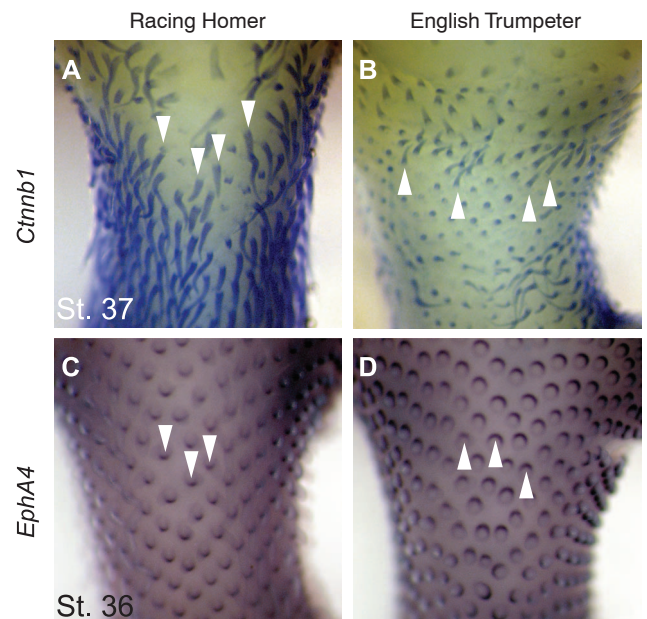
We then used the Variant Annotation, Analysis, and Search Tool [VAASST (18)] to investigate the pigeon genomes for additional coding changes associated with the head crest phenotype. This identified one gene with genome-wide significance: *EphB2*, and specifically the *cr* single-nucleotide polymorphism (SNP) ($P_{\text{genome}} = 2.0 \times 10^{-8}$) (Fig. 2, C and D). The *cr* allele has a predicted charge-changing arginine (basic) to cysteine (polar uncharged) transition in the catalytic

loop of the intracellular tyrosine kinase domain of *EphB2* (Fig. 2E). This amino acid position is invariant among other vertebrates, suggesting strong purifying selection for conserved protein function. The same DLAARN to DLAACN motif change we observe in *EphB2* is sufficient to abrogate kinase activity in human and mouse orthologs of the protein tyrosine kinase ZAP-70, and in both mammals and pigeons the mutant phenotypes are inherited recessively (19). Hence, the pigeon *cr* mutation probably abrogates kinase activity in *EphB2* and disrupts downstream signal propagation, consistent with the high VAASST score for this gene. *EphB2* is therefore a convincing candidate for the *cr* locus of classical pigeon genetics (5–7, 14).

In several wild and domesticated species, the repeated evolution of a derived trait has occurred by selection on the same gene, possibly owing to the repeated selection on the same allele or haplotype (20–22). Similarly, the *cr* SNP is part of a 27.4-kb haplotype that is shared by all crested pigeons, suggesting that the mutation occurred just once and spread to multiple breeds by introgression among domestic breeds, or was selected repeatedly from a standing variant in wild rock pigeons (Fig. 2G and fig. S23; the core haplotype containing the *cr* mutation is reduced to 11 kb when uncrested heterozygotes are included). The only gene present in the shared *cr* haplotype is *EphB2* (Fig. 2D, green bar), although at this time we cannot rule out the presence of regulatory variants that might alter the expression of another gene. Crested members of the toy, fantail, Iranian, Jacobin, and owl breed groups are not more closely related to each other than to uncrested breeds (Fig. 1). Nevertheless, members of these groups had head crests

Fig. 3. Feather bud polarity is reversed in the *cr* mutant.

(A and B) Expression of the feather structural gene *Ctnnb1* reveals the direction of outgrowth of early feather buds. St., Hamburger-Hamilton embryonic stage. (A) Neck and occipital head expression of *Ctnnb1* in an embryo of the uncrested racing homer. Feather buds point downward along the contour of the head and neck (arrowheads). (B) Occipital feather buds point upward in the equivalent region of the crested English trumpeter, indicating morphological reversal of feather orientation. (C and D) Expression of the polarity marker *EphA4* was assayed at an earlier developmental stage to test whether feather placodes, the ectodermal thickenings that give rise to feather buds, are also reversed. (C) Polarity marker *EphA4* is expressed posteriorly (arrowheads) in feather placodes of the racing homer. (D) The polarity of placodes is reversed in the English trumpeter. Expression of *EphB2* in the skin is weak and unpolarized at this stage in both morphs (fig. S26).



hundreds of years ago (14), so some of these introgression events must have occurred in the distant past. Breeds with a wide variety of crest phenotypes share the same derived allele; therefore, allelic variation at the *cr* locus alone does not control all aspects of crest development (14). Other genetic and developmental factors beyond this locus must contribute to variation in crest morphology, akin to the presumed complex genetic architecture of species-level divergence in feather ornaments (2).

In crested pigeons, feather placode polarity and bud outgrowth are inverted during embryogenesis (Fig. 3). Expression of *EphB2* is not polarized in early placodes (fig. S26), so the effects of the *cr* mutation on feather polarity are probably exerted earlier in development. Why might the crest phenotype be limited to the head and neck? In Naked neck chicken mutants, regionalized production of retinoic acid allows uniform up-regulation of *Bmp7* expression to change skin phenotypes in the neck but not the body (23). Similarly, the head crests of several chicken breeds, in which feathers are elongated but do not have a reversed growth trajectory as in pigeons, are localized to the top of the head, probably due to ectopic expression of *Hox* positional cues (24). Together these examples provide evidence for regionalization of the developing head and neck skin in the chicken. We propose that analogous mechanisms might underlie skin regionalization in the pigeon and allow *cr* to change feather polarity in the occiput and neck, but not elsewhere.

Our study of domestic rock pigeons illustrates how combining comparative genomics and population-based analyses forwards our understanding of genetic relationships and the genomic basis of traits. Many of the traits that vary

among pigeon breeds also vary among wild species of birds and other animals (2, 25); thus, pigeons are a model for identifying the genetic basis of variation in traits of general interest. Moreover, variation in many traits in domestic pigeons, including the head crest phenotype described here, is constructive rather than regressive: Breeds derived from the ancestral rock pigeon possess traits that the ancestor does not have. Although adaptive regressive traits are important, the genetic basis of constructive traits in vertebrates remains comparatively poorly understood. The domestic pigeon is thus a promising model with which to explore the genetic architecture of derived, constructive phenotypes in a bird that is amenable to genetic, genomic, and developmental investigation.

References and Notes

1. C. A. Driscoll, D. W. Macdonald, S. J. O'Brien, *Proc. Natl. Acad. Sci. U.S.A.* **106** (suppl. 1), 9971 (2009).
2. T. D. Price, *Genetica* **116**, 311 (2002).
3. C. Darwin, *On the Origin of Species by Means of Natural Selection* (John Murray, London, 1859).
4. C. Darwin, *The Variation of Animals and Plants Under Domestication* (John Murray, London, 1868), vol. 1.
5. T. H. Morgan, *Biol. Bull.* **21**, 215 (1911).
6. A. Sell, *Breeding and Inheritance in Pigeons* (Schober Verlags-GmbH, Hengersberg, Germany, 1994).
7. See the supplementary materials on Science Online.
8. C. N. Balakrishnan, S. V. Edwards, *Genetics* **181**, 645 (2009).
9. H. Ellegren *et al.*, *Nature* **491**, 756 (2012).
10. J. Aerts *et al.*, *Cytogenet. Genome Res.* **117**, 338 (2007).
11. K. P. Johnson *et al.*, *Auk* **118**, 874 (2001).
12. S. A. Stringham *et al.*, *Curr. Biol.* **22**, 302 (2012).
13. D. H. Alexander, J. Novembre, K. Lange, *Genome Res.* **19**, 1655 (2009).
14. W. M. Levi, *The Pigeon* (Levi Publishing, Sumpter, SC, ed. 2 revised, 1986).
15. T. Amundsen, *Trends Ecol. Evol.* **15**, 149 (2000).
16. I. W. McKinnell, H. Makarenkova, I. de Curtis, M. Turmaine, K. Patel, *Dev. Biol.* **270**, 94 (2004).

17. R. N. Kelsh, M. L. Harris, S. Colanesi, C. A. Erickson, *Semin. Cell Dev. Biol.* **20**, 90 (2009).
18. M. Vandell *et al.*, *Genome Res.* **21**, 1529 (2011).
19. M. E. Elder *et al.*, *J. Immunol.* **166**, 656 (2001).
20. P. F. Colosimo *et al.*, *Science* **307**, 1928 (2005).
21. N. B. Sutter *et al.*, *Science* **316**, 112 (2007).
22. A. S. Van Laere *et al.*, *Nature* **425**, 832 (2003).
23. C. Mou *et al.*, *PLoS Biol.* **9**, e1001028 (2011).
24. Y. Wang *et al.*, *PLoS ONE* **7**, e34012 (2012).
25. L. F. Baptista, J. E. Gomez Martinez, H. M. Horblit, *Acta Zoologica Mex.* **25**, 719 (2009).

Acknowledgments: We thank the University of Washington Burke Museum for the *C. rupestris* tissue sample (UWBM 59803); J. Oldham, K. Wright, the Utah Pigeon Club, the National Pigeon Association, and A. and H. O. Christiansen for domestic pigeon samples; D. Clayton for feral samples; and D. Clayton, M. Horvath, D. Kingsley, R. Nielsen, and W. Warren for discussion and comments. Supported by a Burroughs Wellcome Fund Career Award in the Biomedical Sciences, NSF CAREER DEB-1149160, University of Utah Research Foundation (M.D.S.); NIH training grant T32GM007464 (S.A.S.); NIH training grant T32HD07491 (E.T.D.); an NSF EDEN internship (A.I.V.); NIH/NHGRI R01HG004694 and NIH ARRA GO RC2HG005619 (M.Y.); and the Danish National Research Foundation (M.T.P.G. and E.W.). We acknowledge a computer time allocation from the Center for High Performance Computing at the University of Utah. This whole-genome shotgun project has been deposited at DDBJ/EMBL/GenBank under accession no. AKCR00000000 (the first version described here is AKCR01000000; raw reads, SRA052637); RNA-seq data for annotation, accession no. GSE39333; and raw reads for resequenced genomes, accession no. SRA054391.

Supplementary Materials

www.sciencemag.org/cgi/content/full/science.1230422/DC1
Materials and Methods
Supplementary Text
Figs. S1 to S27
Tables S1 to S28
References (26–72)

19 September 2012; accepted 7 December 2012
Published online 31 January 2013;
10.1126/science.1230422

KNOX2 Genes Regulate the Haploid-to-Diploid Morphological Transition in Land Plants

Keiko Sakakibara,^{1,2,3,4*} Sayuri Ando,^{3,4} Hoichong Karen Yip,⁵
Yosuke Tamada,^{4,6} Yuji Hiwatashi,^{4,6†} Takashi Murata,^{4,6} Hironori Deguchi,¹
Mitsuyasu Hasebe,^{3,4,6} John L. Bowman^{2,5*}

Unlike animals, land plants undergo an alternation of generations, producing multicellular bodies in both haploid (1n: gametophyte) and diploid (2n: sporophyte) generations. Plant body plans in each generation are regulated by distinct developmental programs initiated at either meiosis or fertilization, respectively. In mosses, the haploid gametophyte generation is dominant, whereas in vascular plants—including ferns, gymnosperms, and angiosperms—the diploid sporophyte generation is dominant. Deletion of the class 2 KNOTTED1-LIKE HOMEBOX (KNOX2) transcription factors in the moss *Physcomitrella patens* results in the development of gametophyte bodies from diploid embryos without meiosis. Thus, KNOX2 acts to prevent the haploid-specific body plan from developing in the diploid plant body, indicating a critical role for the evolution of KNOX2 in establishing an alternation of generations in land plants.

Plants have a life cycle characterized by alternation between two generations, haploid (gametophyte) and diploid (sporophyte),

where each phase develops a multicellular body (1, 2). The gametophyte produces gametes—sperm (or pollen) and egg cells—and may be the domi-

nant photosynthetic generation, as in liverworts, mosses, and hornworts. The sporophyte produces haploid spores via meiosis and is the dominant photosynthetic generation in the vascular plants. The alternation of generations in land plants results in the possibility that tissue differentiation in each generation is governed by different genetic programs, initiated by either fertilization (haploid to diploid) or meiosis (diploid to haploid). Land plants probably evolved from a freshwater algal ancestor, with a life cycle similar to

¹Department of Biological Science, Graduate School of Science, Hiroshima University, Higashi-Hiroshima 739-8526, Japan. ²School of Biological Sciences, Monash University, Melbourne, Victoria 3800, Australia. ³ERATO, Japan Science and Technology Agency, Okazaki 444-8585, Japan. ⁴National Institute for Basic Biology, Okazaki 444-8585, Japan. ⁵Section of Plant Biology, University of California, Davis, One Shields Avenue, Davis, CA 95616, USA. ⁶School of Life Science, The Graduate University for Advanced Studies, Okazaki 444-8585, Japan.

*To whom correspondence should be addressed. E-mail: john.bowman@monash.edu (J.L.B.); bara@hiroshima-u.ac.jp (K.S.)
†Present address: National Plant Phenomics Centre, Institute of Biological, Environmental and Rural Sciences, Aberystwyth University, Aberystwyth, SY23 3EB, UK.